

Current induced bistability in giant magnetoresistive multilayer thin films

A. Prabhakar

Citation: *Journal of Applied Physics* **99**, 08S306 (2006); doi: 10.1063/1.2172532

View online: <https://doi.org/10.1063/1.2172532>

View Table of Contents: <http://aip.scitation.org/toc/jap/99/8>

Published by the *American Institute of Physics*

Ultra High Performance SDD Detectors



See all our XRF Solutions

Current induced bistability in giant magnetoresistive multilayer thin films

A. Prabhakar^{a)}

Department of Electrical Engineering, Indian Institute of Technology, Chennai 600036, India

(Presented on 3 November 2005; published online 24 April 2006)

The low frequency noise observed in giant magnetoresistive (GMR) sensors exhibited a bistability at certain critical values of bias current. As the sensor oscillated between the two states of a bistable system, the power spectral density (PSD) of the noise showed two peaks; a narrow low frequency peak corresponding to twice the average residence time in a bistable system and a broad high frequency peak corresponding to intrawell vibration. The peaks were visible in the PSD even when the bistability was not pronounced in a time trace. The PSD showed deviations from a Lorentzian behavior indicating that the energy minima and the barrier between them depended on the bias current. A simple analytic model was developed to describe the change in the energy of the system with bias current. The model was based on the physical structure of the sensor and the estimated path of current flow. At particular current induced bias field values, the system was described by multiple energy minima permitting thermal noise excitation of the free layer magnetization. © 2006 American Institute of Physics. [DOI: 10.1063/1.2172532]

I. INTRODUCTION

Noise in magnetoresistive sensors (MR) has been of continuing interest to researchers.^{1,2} Noise has been characterized as $1/f$ type of flicker noise, random telegraph noise (RTN), popcorn noise, and base line noise.³⁻⁶ The name chosen is often reflective of the frequency or time domain measurement process, although the physical mechanism that manifests itself as noise can sometimes be traced to the same source.⁶ Tunnel MR sensors with smaller volumes and higher operating frequencies have a greater susceptibility to failure due to excessive noise.⁷

Evidence of RTN in giant magnetoresistive (GMR) read-back sensors has serious implications to a recording channel and has evoked much attention.^{8,9} There have been attempts to characterize such noise in both the frequency and time domain.^{10,11} However, theoretical attempts to understand this phenomenon have been limited to thermal activation models that predict the energy difference between two states based on their respective lifetimes.^{2,12} Magnetic stochastic resonance (SR) in a bistable system was predicted using the solutions to the Landau-Lifshitz-Gilbert equation.¹³ Recent work on hexagonal spin-valve nanopillars has demonstrated that the spin-momentum transfer can also induce bistability.¹⁴

Studies on RTN have indicated the presence of bistable magnetic states with the residence time in each state being affected by factors such as temperature and defects in the film stacks.^{2,6,15} The bias current in a GMR sensor can be used to localize the magnetic defects to the free or pinned layers of the multilayer stack.¹⁶ We expand this work and use the bias current to vary the magnetic state of the sensor until RTN was observed. The power spectral density (PSD) as a function of bias current showed a peak easily identified as

the characteristic peak for interwell hopping, opening the possibility of explaining base line shifts as a manifestation of stochastic resonance in bistable systems.¹⁷

II. EXPERIMENTAL OBSERVATIONS

The noise traces of an unstable GMR sensor are shown in Fig. 1 for the two cases when the bias currents were 5 and 7 mA. Similar noise traces of 20K samples each were captured with 1 ns sampling time on a Lecroy LC574AL digital oscilloscope as the head was flying on a spin stand. The bias current to the device was increased from 5 to 9 mA. The noise reached its maximum peak to peak amplitude at a bias current of 7 mA. Despite the noise trace showing evidence of RTN, its variance when calculated using the voltages in one metastable state showed no appreciable difference in value.

The PSD of the noise with increasing bias current is shown in Fig. 2 along with a $1/f$ curve provided as a reference. The activation peak identified corresponding to intrawell vibration is evident even at 5 and 9 mA of bias cur-

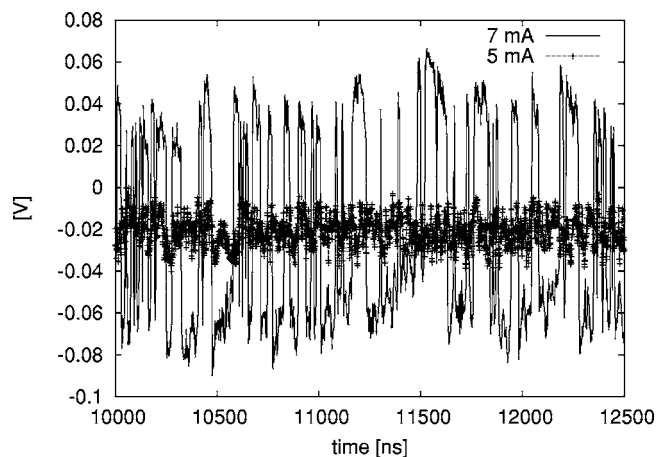


FIG. 1. Noise traces of the GMR sensor. The noise is similar for 5 and 9 mA of bias current.

^{a)}Electronic mail: anilpr@iit.ac.in

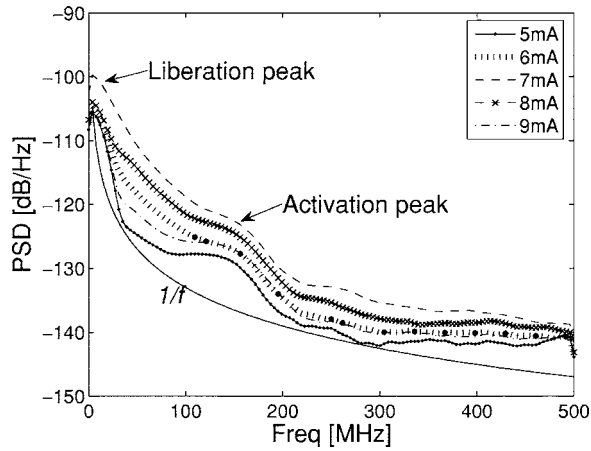


FIG. 2. Power spectral density of noise as a function of increasing bias current. The $1/f$ noise is as a reference.

rent, when there was no evidence of RTN in the noise trace. The low frequency peak corresponds to interwell hopping and is appropriately named the liberation peak. Thus the PSD manages to effectively capture the bistable nature of the sensor even when the difference between the energy states is minimal. The frequency of the liberation peak around 3 MHz corresponds to approximately twice the average residence time of $0.2 \mu\text{s}$ that was observed from the noise trace with the 7 mA bias current. The primary difference between this experiment and other works where the Arrhenius model is used to describe RTN is that the bistability appears to be triggered by a change in bias current. Since the noise variance in one state does not appear to increase significantly with increasing current, it is unlikely that the bistability is solely a manifestation of an increase in temperature.

When the residence times in the two states of a bistable system are equal but independent of each other, we expect the PSD to have the Lorentzian form¹⁴

$$S(\omega) = \frac{\Delta V}{4\pi} \frac{1}{1 + \omega^2 \tau^2}, \quad (1)$$

where $\tau \approx 0.2 \mu\text{s}$ is the average residence time. Since the observed PSD does not follow a simple Lorentzian behavior, we infer that the energy of the states and the potential barrier between them inhibiting fluctuations are functions of the current induced bias field.

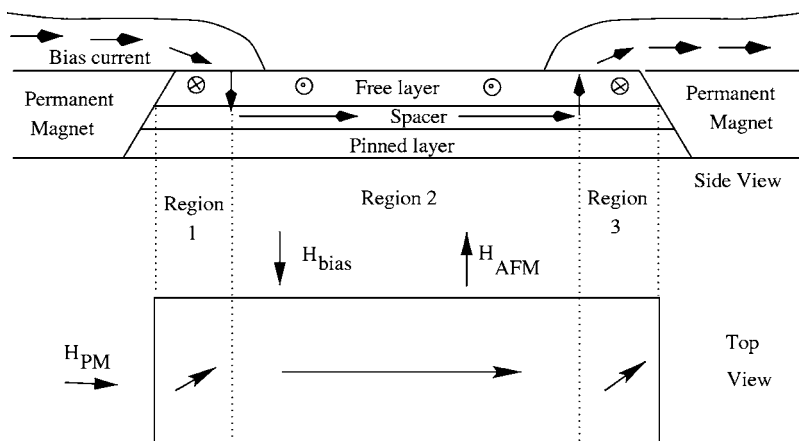


FIG. 3. Schematic of the device. The side view shows the estimated path of the bias current (arrows) and the associated bias magnetic field (circles). The top view shows a simplified spatial distribution of the magnetization.

III. CURRENT INDUCED BISTABILITY

In the simplest possible model for the GMR element in a recording head, the multilayer film stack is reduced to three layers consisting of a free layer (which rotates on the application of an external field), a spacer layer (usually Cu), and a pinned layer (usually coupled to an antiferromagnet). A current is applied to the film stack via leads that form an overlay at the sides of the film stack. While the GMR effect depends on the relative distribution of the spin-dependent conduction electrons in the film stack, it is often assumed that most of the current flows through the Cu spacer layer which has the highest conductivity. By neglecting the magnetoresistive effects of the multilayers, we obtained a first approximation to the path taken by the bias current. The approximate path was determined using a finite-element software package and is shown by the arrows in the side view of the device. The bias magnetic field associated with this current lies in the plane of the film. Note that voltage across the device, to lowest order, is determined by the magnetization of the central part of the free layer (region 2) while the edges of the free layer (regions 1 and 3) have second order contributions. Hence, we assumed that the optimal bias current (I_b) is chosen such that the magnetization in region 2 is parallel to the easy axis of the film, as shown in Fig. 3.

Consider the case of three magnetization vectors ($\vec{M}_i, i=1, 2, 3$) coupled to each other via a magnetostatic interaction (E_D) as well as an exchange interaction (E_J) between adjacent neighbors, such that

$$E_D = - \sum_{i=1}^3 \vec{M}_i \left[\sum_{j \neq i} \vec{D}_{ij} \cdot \vec{M}_j + \frac{1}{2} \vec{D}_{ii} \cdot \vec{M}_i \right], \quad (2)$$

$$E_J = -J[\vec{M}_1 \cdot \vec{M}_2 + \vec{M}_2 \cdot \vec{M}_3], \quad (3)$$

where \vec{D}_{ij} is a magnetostatic interaction matrix between the i th and the j th magnetization and J is the exchange coupling between nearest neighbors. The total energy of the system is obtained by adding the contributions from anisotropy (E_A) and the external magnetic field (E_H),

$$E_A = K \sum_{i=1}^3 \sin^2 \theta_i, \quad (4)$$

$$E_H = - \sum_{i=1}^3 \bar{H}_i \cdot \bar{M}_i, \quad (5)$$

with K being the anisotropy constant, θ_i being the angle \bar{M}_i relative to the easy axis direction, and \bar{H}_i being the external magnetic field in each region. The external magnetic field can be split into contributions from a permanent magnet (PM), the antiferromagnetic pinned layer (AFM), and the bias current, written as

$$\bar{H}_{\text{bias}}^{(i)} = \bar{H}_{\text{PM}} + \bar{H}_{\text{AFM}} + \bar{H}_i(I). \quad (6)$$

Finally, the total energy $E = E_D + E_J + E_A + E_H$. Using an ϵ -series expansion of the form $\theta_i = \epsilon \phi_i$, we can easily show that the energy terms of $O(\epsilon^0)$ and $O(\epsilon^1)$ are merely additive constants while those with h are $O(\epsilon^2)$. Furthermore, assuming that the magnetization in each region is largely parallel to the uniaxial direction i.e., $\theta_i \rightarrow 0$ i , it was possible to simplify the calculation of the demagnetization tensor. We describe the demagnetization as

$$\bar{M}_j \bar{D} \cdot \bar{M}_i \approx M_i M_j \cos \theta_i \cos \theta_j. \quad (7)$$

As h increases, the energy diagram for $E(\theta_2)$ takes the form of a double well potential between the two stable states. Figure 4 is a top view of the free layer showing the two possible states at a critical bias field (h_c). Analytic solutions for h_c were obtained by looking for solutions to

$$\frac{dE}{d\theta_2} = \sum_{i=1}^3 \frac{\partial E}{\partial \theta_i} \frac{d\theta_i}{d\theta_2} \approx \frac{\partial E}{\partial \theta_2} = 0. \quad (8)$$

Since we focused on finding the bistable states for the magnetization \bar{M}_2 , we assumed that \bar{M}_1 and \bar{M}_3 remained unchanged and hence $d\theta_1/d\theta_2 = d\theta_3/d\theta_2 = 0$. The assumption of a plane of symmetry down the center of the device allowed us to set $M_1 = M_3, D_{12} = D_{23}$, and define $J' = M_2(2JM_1 - H_{\text{PM}})$. With these substitutions and as $\theta_{1,3} \rightarrow 0$, we obtained the transcendental equation

$$2K \sin \theta_2 \cos \theta_2 - J' \sin \theta_2 + h_2 M_2 \cos \theta_2 = 0. \quad (9)$$

Using $\tan \theta_2 \approx \theta_2 + \theta_2^3/3$, we obtain

$$a\theta_2^3 - b\theta_2 + h_2 = 0, \quad (10)$$

where

$$a \triangleq \frac{2K}{M_2} - \frac{J'}{M_2} \quad (11)$$

and

$$b \triangleq \frac{K}{3M_2} + \frac{J'}{3M_2}. \quad (12)$$

The stability of the cubic roots is determined by

$$Q(h_2) \triangleq \left(\frac{-b}{a}\right)^3 + \left(\frac{h_2}{a}\right)^2, \quad (13)$$

with three real and unequal solutions existing when $Q < 0$ and two of them being equal for $Q = 0$. Consequently, h_c was defined by $Q(h_c) = 0$ and was estimated as

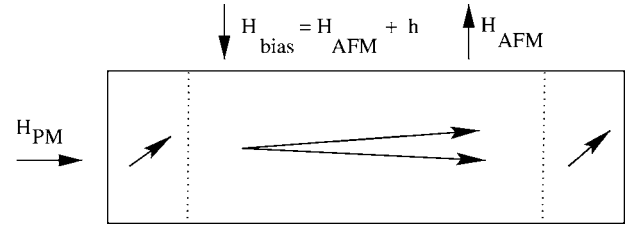


FIG. 4. Top view of the device showing the two possible states for the magnetization at the center of the when the excess field due to the bias current ($h = H_{\text{bias}}^{(2)} - H_{\text{AFM}}$) is less than its critical value (h_c).

$$h_c = \frac{1}{M_2} \sqrt{2K - J'} \left(\frac{K}{3} + J' \right)^{3/2}. \quad (14)$$

If the field from the permanent magnet is weak such that $J' < 2K$, we obtain a real value for the critical field at which the sensor exhibits bistability.

IV. SUMMARY

Bistability in a GMR sensor was observed to be dependent on the bias current applied to the device. The power spectral density of the noise traces shows a deviation from Lorentzian behavior with a peak below 5 MHz corresponding to interwell oscillation and a broad peak around 150 MHz corresponding to intra well vibration. These peaks are visible even when the time series noise traces do not clearly exhibit bistability. Hence, the PSD can be used as an effective tool to characterize current induced instability in the sensor. A simple analytic model to explain the current induced bistability was developed. For sensors with weak permanent magnet fields, the model yielded an approximate critical field at which the magnetization of the free layer had multiple energy minima. The model can be used for further studies in an effort to relate experimentally observable base line shifts to stochastic resonance in bistable magnetic sensors.

¹A. Wallash, IEEE Trans. Magn. **34**, 1450 (1998).

²H. T. Hardner, M. J. Hurben, and N. Tabat, IEEE Trans. Magn. **35**, 2592 (1999).

³H. Wan, M. M. Bohlinger, M. Jenson, and A. Hurst, IEEE Trans. Magn. **33**, 3409 (1997).

⁴M. Xiao, K. B. Klaassen, and J. C. L. van Peppen, IEEE Trans. Magn. **36**, 2593 (2000).

⁵B. R. Baker, IEEE Trans. Magn. **35**, 2583 (1999).

⁶L. Chen *et al.*, IEEE Trans. Magn. **37**, 1343 (2001).

⁷K. B. Klaassen, J. C. L. van Peppen, and X. Xing, J. Appl. Phys. **93**, 8573 (2003).

⁸D. S. L. Zhong, J. Giusti, and J. F. de Castro, IEEE Trans. Magn. **36**, 2587 (2000).

⁹J. Zhang *et al.*, IEEE Trans. Magn. **37**, 1678 (2000).

¹⁰Y. Hsu, IEEE Trans. Magn. **31**, 2636 (1995).

¹¹A. Prabhakar and J. Zhang, IEEE Trans. Magn. **36**, 3621 (2000).

¹²L. Kirschenbaum, C. T. Rogers, S. E. Russek, and S. C. Sanders, IEEE Trans. Magn. **31**, 3942 (1995).

¹³A. N. Grigorenko and P. Nikitin, IEEE Trans. Magn. **31**, 2491 (1995).

¹⁴M. R. Pufall *et al.*, Phys. Rev. B **69**, 214409 (2004).

¹⁵L. Chen *et al.*, IEEE Trans. Magn. **36**, 3195 (2000).

¹⁶H. T. Hardner, IEEE Trans. Magn. **36**, 2584 (2000).

¹⁷L. Alfonsi, L. Gammaitoni, S. Santucci, and A. R. Bulsara, Phys. Rev. E **62**, 299 (2000).